FERMILAB-PUB-07-042-E

Observation of WZ Production

A. Abulencia,[24] J. Adelman,[13] T. Affolder,[10] T. Akimoto,[56] M.G. Albrow,[17] D. Ambrose,[17] S. Amerio,[44] D. Amidei,[35] A. Anastassov,[53] K. Anikeev,[17] A. Annovi,[19] J. Antos,[14] M. Aoki,[56] G. Apollinari,[17] J.-F. Arguin,[34] T. Arisawa,[58] A. Artikov,[15] W. Ashmanskas,[17] A. Attal,[8] F. Azfar,[43] P. Azzi-Bacchetta,[44] P. Azzurri,[47] N. Bacchetta,[44] W. Badgett,[17] A. Barbaro-Galtieri,[29] V.E. Barnes,[49] B.A. Barnett,[25] S. Baroiant,[7] V. Bartsch,[31] G. Bauer,[33] F. Bedeschi,[47] S. Behari,[25] S. Belforte,[55] G. Bellettini,[47] J. Bellinger,[60] A. Belloni,[33] D. Benjamin,[16] A. Beretvas,[17] J. Beringer,[29] T. Berry,[30] A. Bhatti,[51] M. Binkley,[17] D. Bisello,[44] R.E. Blair,[2] C. Blocker,[6] B. Blumenfeld,[25] A. Bocci,[16] A. Bodek,[50] V. Boisvert,[50] G. Bolla,[49] A. Bolshov,[33] D. Bortoletto,[49] J. Boudreau,[48] A. Boveia,[10] B. Brau,[10] L. Brigliadori,[5] C. Bromberg,[36] E. Brubaker,[13] J. Budagov,[15] H.S. Budd,[50] S. Budd,[24] S. Budroni,[47] K. Burkett,[17] G. Busetto,[44] P. Bussey,[21] K. L. Byrum,[2] S. Cabrera^{o},[16] M. Campanelli,[20] M. Campbell,[35] F. Canelli,[17] A. Canepa,[49] S. Carillo^{i},[18] D. Carlsmith,[60] R. Carosi,[47] S. Carron,[34] M. Casarsa,[55] A. Castro,[5] P. Catastini,[47] D. Cauz,[55] M. Cavalli-Sforza,[3] A. Cerri,[29] L. Cerrito^{m},[43] S.H. Chang,[28] Y.C. Chen,[1] M. Chertok,[7] G. Chiarelli,[47] G. Chlachidze,[15] F. Chlebana,[17] I. Cho,[28] K. Cho,[28] D. Chokheli,[15] J.P. Chou,[22] G. Choudalakis,[33] S.H. Chuang,[60] K. Chung,[12] W.H. Chung,[60] Y.S. Chung,[50] M. Ciljak,[47] C.I. Ciobanu,[24] M.A. Ciocci,[47] A. Clark,[20] D. Clark,[6] M. Coca,[16] G. Compostella,[44] M.E. Convery,[51] J. Conway,[7] B. Cooper,[36] K. Copic,[35] M. Cordelli,[19] G. Cortiana,[44] F. Crescioli,[47] C. Cuenca Almenar^{o},[7] J. Cuevas^{l},[11] R. Culbertson,[17] J.C. Cully,[35] D. Cyr,[60] S. DaRonco,[44] M. Datta,[17] S. D'Auria,[21] T. Davies,[21] M. D'Onofrio,[3] D. Dagenhart,[6] P. de Barbaro,[50] S. De Cecco,[52] A. Deisher,[29] G. De Lentdecker^{c},[50] M. Dell'Orso,[47] F. Delli Paoli,[44] L. Demortier,[51] J. Deng,[16] M. Deninno,[5] D. De Pedis,[52] P.F. Derwent,[17] G.P. Di Giovanni,[45] C. Dionisi,[52] B. Di Ruzza,[55] J.R. Dittmann,[4] P. DiTuro,[53] C. Dörr,[26] S. Donati,[47] M. Donega,[20] P. Dong,[8] J. Donini,[44] T. Dorigo,[44] S. Dube,[53] J. Efron,[40] R. Erbacher,[7] D. Errede,[24] S. Errede,[24] R. Eusebi,[17] H.C. Fang,[29] S. Farrington,[30] I. Fedorko,[47] W.T. Fedorko,[13] R.G. Feild,[61] M. Feindt,[26] J.P. Fernandez,[32] R. Field,[18] G. Flanagan,[49] A. Foland,[22] S. Forrester,[7] G.W. Foster,[17] M. Franklin,[22] J.C. Freeman,[29] I. Furic,[13] M. Gallinaro,[51] J. Galyardt,[12] J.E. Garcia,[47] F. Garberson,[10] A.F. Garfinkel,[49] C. Gay,[61] H. Gerberich,[24] D. Gerdes,[35] S. Giagu,[52] P. Giannetti,[47] A. Gibson,[29] K. Gibson,[48] J.L. Gimmell,[50] C. Ginsburg,[17] N. Giokaris^{a},[15] M. Giordani,[55] P. Giromini,[19] M. Giunta,[47] G. Giurgiu,[12] V. Glagolev,[15] D. Glenzinski,[17] M. Gold,[38] N. Goldschmidt,[18] J. Goldstein^{b},[43] A. Golossanov,[17] G. Gomez,[11] G. Gomez-Ceballos,[11] M. Goncharov,[54] O. González,[32] I. Gorelov,[38] A.T. Goshaw,[16] K. Goulianos,[51] A. Gresele,[44] M. Griffiths,[30] S. Grinstein,[22] C. Grosso-Pilcher,[13] R.C. Group,[18] U. Grundler,[24] J. Guimaraes da Costa,[22] Z. Gunay-Unalan,[36] C. Haber,[29] K. Hahn,[33] S.R. Hahn,[17] E. Halkiadakis,[53] A. Hamilton,[34] B.-Y. Han,[50] J.Y. Han,[50] R. Handler,[60] F. Happacher,[19] K. Hara,[56] M. Hare,[57] S. Harper,[43] R.F. Harr,[59] R.M. Harris,[17] M. Hartz,[48] K. Hatakeyama,[51] J. Hauser,[8] A. Heijboer,[46] B. Heinemann,[30] J. Heinrich,[46] C. Henderson,[33] M. Herndon,[60] J. Heuser,[26] D. Hidas,[16] C.S. Hill^{b},[10] D. Hirschbuehl,[26] A. Hocker,[17] A. Holloway,[22] S. Hou,[1] M. Houlden,[30] S.-C. Hsu,[9] B.T. Huffman,[43] R.E. Hughes,[40] U. Husemann,[61] J. Huston,[36] J. Incandela,[10] G. Introzzi,[47] M. Iori,[52] Y. Ishizawa,[56] A. Ivanov,[7] B. Iyutin,[33] E. James,[17] D. Jang,[53] B. Jayatilaka,[35] D. Jeans,[52] H. Jensen,[17] E.J. Jeon,[28] S. Jindariani,[18] M. Jones,[49] K.K. Joo,[28] S.Y. Jun,[12] J.E. Jung,[28] T.R. Junk,[24] T. Kamon,[54] P.E. Karchin,[59] Y. Kato,[42] Y. Kemp,[26] R. Kephart,[17] U. Kerzel,[26] V. Khotilovich,[54] B. Kilminster,[40] D.H. Kim,[28] H.S. Kim,[28] J.E. Kim,[28] M.J. Kim,[12] S.B. Kim,[28] S.H. Kim,[56] Y.K. Kim,[13] N. Kimura,[56] L. Kirsch,[6] S. Klimenko,[18] M. Klute,[33] B. Knuteson,[33] B.R. Ko,[16] K. Kondo,[58] D.J. Kong,[28] J. Konigsberg,[18] A. Korytov,[18] A.V. Kotwal,[16] A. Kovalev,[46] A.C. Kraan,[46] J. Kraus,[24] I. Kravchenko,[33] M. Kreps,[26] J. Kroll,[46] N. Krumnack,[4] M. Kruse,[16] V. Krutelyov,[10] T. Kubo,[56] S. E. Kuhlmann,[2] T. Kuhr,[26] Y. Kusakabe,[58] S. Kwang,[13] A.T. Laasanen,[49] S. Lai,[34] S. Lami,[47] S. Lammel,[17] M. Lancaster,[31] R.L. Lander,[7] K. Lannon,[40] A. Lath,[53] G. Latino,[47] I. Lazzizzera,[44] T. LeCompte,[2] J. Lee,[50] J. Lee,[28] Y.J. Lee,[28] S.W. Lee^{n},[54] R. Lefèvre,[3] N. Leonardo,[33] S. Leone,[47] S. Levy,[13] J.D. Lewis,[17] C. Lin,[61] C.S. Lin,[17] M. Lindgren,[17] E. Lipeles,[9] A. Lister,[7] D.O. Litvintsev,[17] T. Liu,[17] N.S. Lockyer,[46] A. Loginov,[61] M. Loreti,[44] P. Loverre,[52] R.-S. Lu,[1] D. Lucchesi,[44] P. Lujan,[29] P. Lukens,[17] G. Lungu,[18] L. Lyons,[43] J. Lys,[29] R. Lysak,[14] E. Lytken,[49] P. Mack,[26] D. MacQueen,[34] R. Madrak,[17] K. Maeshima,[17] K. Makhoul,[33] T. Maki,[23] P. Maksimovic,[25] S. Malde,[43] G. Manca,[30] F. Margaroli,[5] R. Marginean,[17] C. Marino,[26] C.P. Marino,[24] A. Martin,[61] M. Martin,[25] V. Martin^{g},[21] M. Martínez,[3] T. Maruyama,[56] P. Mastrandrea,[52] T. Masubuchi,[56] H. Matsunaga,[56] M.E. Mattson,[59] R. Mazini,[34] P. Mazzanti,[5] K. McCarthy,[9] K.S. McFarland,[50] P. McIntyre,[54] R. McNulty^{f},[30] A. Mehta,[30] P. Mehtala,[23] S. Menzemer^{h},[11] A. Menzione,[47] P. Merkel,[49] C. Mesropian,[51] A. Messina,[36] T. Miao,[17] N. Miladinovic,[6] J. Miles,[33] R. Miller,[36] C. Mills,[10] M. Milnik,[26] A. Mitra,[1] G. Mitselmakher,[18] A. Miyamoto,[27] S. Moed,[20] N. Moggi,[5]

B. Mohr,[8] R. Moore,[17] M. Morello,[47] P. Movilla Fernandez,[29] J. Mülmenstädt,[29] A. Mukherjee,[17] Th. Muller,[26] R. Mumford,[25] P. Murat,[17] J. Nachtman,[17] A. Nagano,[56] J. Naganoma,[58] I. Nakano,[41] A. Napier,[57] V. Necula,[18] C. Neu,[46] M.S. Neubauer,[9] J. Nielsen,[29] T. Nigmanov,[48] L. Nodulman,[2] O. Norniella,[3] E. Nurse,[31] S.H. Oh,[16] Y.D. Oh,[28] I. Oksuzian,[18] T. Okusawa,[42] R. Oldeman,[30] R. Orava,[23] K. Osterberg,[23] C. Pagliarone,[47] E. Palencia,[11] V. Papadimitriou,[17] A.A. Paramonov,[13] B. Parks,[40] S. Pashapour,[34] J. Patrick,[17] G. Pauletta,[55] M. Paulini,[12] C. Paus,[33] D.E. Pellett,[7] A. Penzo,[55] T.J. Phillips,[16] G. Piacentino,[47] J. Piedra,[45] L. Pinera,[18] K. Pitts,[24] C. Plager,[8] L. Pondrom,[60] X. Portell,[3] O. Poukhov,[15] N. Pounder,[43] F. Prakoshyn,[15] A. Pronko,[17] J. Proudfoot,[2] F. Ptohos[e],[19] G. Punzi,[47] J. Pursley,[25] J. Rademacker[b],[43] A. Rahaman,[48] N. Ranjan,[49] S. Rappoccio,[22] B. Reisert,[17] V. Rekovic,[38] P. Renton,[43] M. Rescigno,[52] S. Richter,[26] F. Rimondi,[5] L. Ristori,[47] A. Robson,[21] T. Rodrigo,[11] E. Rogers,[24] S. Rolli,[57] R. Roser,[17] M. Rossi,[55] R. Rossin,[18] A. Ruiz,[11] J. Russ,[12] V. Rusu,[13] H. Saarikko,[23] S. Sabik,[34] A. Safonov,[54] W.K. Sakumoto,[50] G. Salamanna,[52] O. Saltó,[3] D. Saltzberg,[8] C. Sánchez,[3] L. Santi,[55] S. Sarkar,[52] L. Sartori,[47] K. Sato,[17] P. Savard,[34] A. Savoy-Navarro,[45] T. Scheidle,[26] P. Schlabach,[17] E.E. Schmidt,[17] M.P. Schmidt,[61] M. Schmitt,[39] T. Schwarz,[7] L. Scodellaro,[11] A.L. Scott,[10] A. Scribano,[47] F. Scuri,[47] A. Sedov,[49] S. Seidel,[38] Y. Seiya,[42] A. Semenov,[15] L. Sexton-Kennedy,[17] A. Sfyrla,[20] M.D. Shapiro,[29] T. Shears,[30] P.F. Shepard,[48] D. Sherman,[22] M. Shimojima[k],[56] M. Shochet,[13] Y. Shon,[60] I. Shreyber,[37] A. Sidoti,[47] P. Sinervo,[34] A. Sisakyan,[15] J. Sjolin,[43] A.J. Slaughter,[17] J. Slaunwhite,[40] K. Sliwa,[57] J.R. Smith,[7] F.D. Snider,[17] R. Snihur,[34] M. Soderberg,[35] A. Soha,[7] S. Somalwar,[53] V. Sorin,[36] J. Spalding,[17] F. Spinella,[47] T. Spreitzer,[34] P. Squillacioti,[47] M. Stanitzki,[61] A. Staveris-Polykalas,[47] R. St. Denis,[21] B. Stelzer,[8] O. Stelzer-Chilton,[43] D. Stentz,[39] J. Strologas,[38] D. Stuart,[10] J.S. Suh,[28] A. Sukhanov,[18] H. Sun,[57] T. Suzuki,[56] A. Taffard,[24] R. Takashima,[41] Y. Takeuchi,[56] K. Takikawa,[56] M. Tanaka,[2] R. Tanaka,[41] M. Tecchio,[35] P.K. Teng,[1] K. Terashi,[51] J. Thom[d],[17] A.S. Thompson,[21] E. Thomson,[46] P. Tipton,[61] V. Tiwari,[12] S. Tkaczyk,[17] D. Toback,[54] S. Tokar,[14] K. Tollefson,[36] T. Tomura,[56] D. Tonelli,[47] S. Torre,[19] D. Torretta,[17] S. Tourneur,[45] W. Trischuk,[34] R. Tsuchiya,[58] S. Tsuno,[41] N. Turini,[47] F. Ukegawa,[56] T. Unverhau,[21] S. Uozumi,[56] D. Usynin,[46] S. Vallecorsa,[20] R. Vanguri,[9] N. van Remortel,[23] A. Varganov,[35] E. Vataga,[38] F. Vázquez[i],[18] G. Velev,[17] G. Veramendi,[24] V. Veszpremi,[49] R. Vidal,[17] I. Vila,[11] R. Vilar,[11] T. Vine,[31] I. Vollrath,[34] I. Volobouev[n],[29] G. Volpi,[47] F. Würthwein,[9] P. Wagner,[54] R.G. Wagner,[2] R.L. Wagner,[17] J. Wagner,[26] W. Wagner,[26] R. Wallny,[8] S.M. Wang,[1] A. Warburton,[34] S. Waschke,[21] D. Waters,[31] M. Weinberger,[54] W.C. Wester III,[17] B. Whitehouse,[57] D. Whiteson,[46] A.B. Wicklund,[2] E. Wicklund,[17] G. Williams,[34] H.H. Williams,[46] P. Wilson,[17] B.L. Winer,[40] P. Wittich[d],[17] S. Wolbers,[17] C. Wolfe,[13] T. Wright,[35] X. Wu,[20] S.M. Wynne,[30] A. Yagil,[9] K. Yamamoto,[42] J. Yamaoka,[53] T. Yamashita,[41] C. Yang,[61] U.K. Yang[j],[13] Y.C. Yang,[28] W.M. Yao,[29] G.P. Yeh,[17] J. Yoh,[17] K. Yorita,[13] T. Yoshida,[42] G.B. Yu,[50] I. Yu,[28] S.S. Yu,[17] J.C. Yun,[17] L. Zanello,[52] A. Zanetti,[55] I. Zaw,[22] X. Zhang,[24] J. Zhou,[53] and S. Zucchelli[5]

(CDF Collaboration*)

[1] *Institute of Physics, Academia Sinica, Taipei, Taiwan 11529, Republic of China*
[2] *Argonne National Laboratory, Argonne, Illinois 60439*
[3] *Institut de Fisica d'Altes Energies, Universitat Autonoma de Barcelona, E-08193, Bellaterra (Barcelona), Spain*
[4] *Baylor University, Waco, Texas 76798*
[5] *Istituto Nazionale di Fisica Nucleare, University of Bologna, I-40127 Bologna, Italy*
[6] *Brandeis University, Waltham, Massachusetts 02254*
[7] *University of California, Davis, Davis, California 95616*
[8] *University of California, Los Angeles, Los Angeles, California 90024*
[9] *University of California, San Diego, La Jolla, California 92093*
[10] *University of California, Santa Barbara, Santa Barbara, California 93106*
[11] *Instituto de Fisica de Cantabria, CSIC-University of Cantabria, 39005 Santander, Spain*
[12] *Carnegie Mellon University, Pittsburgh, PA 15213*
[13] *Enrico Fermi Institute, University of Chicago, Chicago, Illinois 60637*
[14] *Comenius University, 842 48 Bratislava, Slovakia; Institute of Experimental Physics, 040 01 Kosice, Slovakia*
[15] *Joint Institute for Nuclear Research, RU-141980 Dubna, Russia*
[16] *Duke University, Durham, North Carolina 27708*
[17] *Fermi National Accelerator Laboratory, Batavia, Illinois 60510*
[18] *University of Florida, Gainesville, Florida 32611*
[19] *Laboratori Nazionali di Frascati, Istituto Nazionale di Fisica Nucleare, I-00044 Frascati, Italy*
[20] *University of Geneva, CH-1211 Geneva 4, Switzerland*
[21] *Glasgow University, Glasgow G12 8QQ, United Kingdom*
[22] *Harvard University, Cambridge, Massachusetts 02138*
[23] *Division of High Energy Physics, Department of Physics,*
University of Helsinki and Helsinki Institute of Physics, FIN-00014, Helsinki, Finland

[24] University of Illinois, Urbana, Illinois 61801
[25] The Johns Hopkins University, Baltimore, Maryland 21218
[26] Institut für Experimentelle Kernphysik, Universität Karlsruhe, 76128 Karlsruhe, Germany
[27] High Energy Accelerator Research Organization (KEK), Tsukuba, Ibaraki 305, Japan
[28] Center for High Energy Physics: Kyungpook National University, Taegu 702-701, Korea; Seoul National University, Seoul 151-742, Korea; and SungKyunKwan University, Suwon 440-746, Korea
[29] Ernest Orlando Lawrence Berkeley National Laboratory, Berkeley, California 94720
[30] University of Liverpool, Liverpool L69 7ZE, United Kingdom
[31] University College London, London WC1E 6BT, United Kingdom
[32] Centro de Investigaciones Energeticas Medioambientales y Tecnologicas, E-28040 Madrid, Spain
[33] Massachusetts Institute of Technology, Cambridge, Massachusetts 02139
[34] Institute of Particle Physics: McGill University, Montréal, Canada H3A 2T8; and University of Toronto, Toronto, Canada M5S 1A7
[35] University of Michigan, Ann Arbor, Michigan 48109
[36] Michigan State University, East Lansing, Michigan 48824
[37] Institution for Theoretical and Experimental Physics, ITEP, Moscow 117259, Russia
[38] University of New Mexico, Albuquerque, New Mexico 87131
[39] Northwestern University, Evanston, Illinois 60208
[40] The Ohio State University, Columbus, Ohio 43210
[41] Okayama University, Okayama 700-8530, Japan
[42] Osaka City University, Osaka 588, Japan
[43] University of Oxford, Oxford OX1 3RH, United Kingdom
[44] University of Padova, Istituto Nazionale di Fisica Nucleare, Sezione di Padova-Trento, I-35131 Padova, Italy
[45] LPNHE, Universite Pierre et Marie Curie/IN2P3-CNRS, UMR7585, Paris, F-75252 France
[46] University of Pennsylvania, Philadelphia, Pennsylvania 19104
[47] Istituto Nazionale di Fisica Nucleare Pisa, Universities of Pisa, Siena and Scuola Normale Superiore, I-56127 Pisa, Italy
[48] University of Pittsburgh, Pittsburgh, Pennsylvania 15260
[49] Purdue University, West Lafayette, Indiana 47907
[50] University of Rochester, Rochester, New York 14627
[51] The Rockefeller University, New York, New York 10021
[52] Istituto Nazionale di Fisica Nucleare, Sezione di Roma 1, University of Rome "La Sapienza," I-00185 Roma, Italy
[53] Rutgers University, Piscataway, New Jersey 08855
[54] Texas A&M University, College Station, Texas 77843
[55] Istituto Nazionale di Fisica Nucleare, University of Trieste/ Udine, Italy
[56] University of Tsukuba, Tsukuba, Ibaraki 305, Japan
[57] Tufts University, Medford, Massachusetts 02155
[58] Waseda University, Tokyo 169, Japan
[59] Wayne State University, Detroit, Michigan 48201
[60] University of Wisconsin, Madison, Wisconsin 53706
[61] Yale University, New Haven, Connecticut 06520

We report the first observation of the associated production of a W boson and a Z boson. This result is based on 1.1 fb^{-1} of integrated luminosity from $p\overline{p}$ collisions at $\sqrt{s} = 1.96$ TeV collected with the CDF II detector at the Fermilab Tevatron. We observe 16 WZ candidates passing our event selection with an expected background of 2.7 ± 0.4 events. A fit to the missing transverse energy distribution indicates an excess of events compared to the background expectation corresponding to a significance equivalent to six standard deviations. The measured cross section is $\sigma(p\overline{p} \to WZ) = 5.0^{+1.8}_{-1.6}$ pb, consistent with the standard model expectation.

PACS numbers: 12.15.Ji 13.40.Em 13.87.Ce 14.70.Fm 14.70.Hp

The W and Z vector bosons which mediate the weak

*With visitors from [a]University of Athens, [b]University of Bristol, [c]University Libre de Bruxelles, [d]Cornell University, [e]University of Cyprus, [f]University of Dublin, [g]University of Edinburgh, [h]University of Heidelberg, [i]Universidad Iberoamericana, [j]University of Manchester, [k]Nagasaki Institute of Applied Science, [l]University de Oviedo, [m]University of London, Queen Mary and Westfield College, [n]Texas Tech University, [o]IFIC(CSIC-Universitat de Valencia),

interaction are produced individually in large numbers in $p\overline{p}$ collisions at the Fermilab Tevatron, and their cross sections have been measured with high precision [1]. The production of heavy vector boson pairs (WW, WZ, and ZZ) is far less common and can involve the triple gauge couplings (TGCs) between the bosons themselves via an intermediate virtual boson. Deviations of measured diboson production properties from standard model (SM) predictions could arise from new interactions or loop effects due to new particles at energy scales not directly accessible to a given experiment [2]. At the Tevatron, TGCs are probed at the highest energy scales yet achieved.

In this Letter, we report the first observation of WZ production. The production is observed in $p\overline{p}$ collisions at $\sqrt{s} = 1.96$ TeV using 1.1 fb^{-1} of integrated luminosity collected by the CDF II detector at the Fermilab Tevatron. We consider the decay channel $WZ \to \ell'\nu_{\ell'}\ell\ell$, where ℓ' and ℓ are electrons or muons directly from W and Z decay, respectively, or from the leptonic decay of τ's when one or both vector bosons decay to τ leptons.

The most sensitive previous search for WZ production was reported by the DØ Collaboration using 0.3 fb^{-1} of integrated luminosity, where three $WZ \to \ell'\nu_{\ell'}\ell\ell$ candidate events were found [3]. The observed events had a probability of 3.5% to be due to background fluctuations, corresponding to $\sigma(WZ) < 13.3$ pb at 95% C.L. A search for the sum of WZ and ZZ production in decays to 2, 3, and 4 lepton channels by the CDF Collaboration using 0.194 fb^{-1} of integrated luminosity determined that $\sigma(WZ + ZZ) < 15.2$ pb at 95% C.L. [4]. The next-to-leading order (NLO) WZ cross section prediction for $p\overline{p}$ collisions at $\sqrt{s} = 1.96$ TeV is 3.7 ± 0.3 pb [5].

The components of the CDF II detector relevant to this analysis are described briefly here; a more complete description can be found elsewhere [6]. The detector geometry is described using the azimuthal angle ϕ and the pseudorapidity $\eta \equiv -\ln[\tan(\theta/2)]$, where θ is the polar angle with respect to the proton beam axis (positive z-axis). The pseudorapidity of a particle originating from the center of the detector is referred to as $\eta_{\rm d}$.

The trajectories of charged particles (tracks) are reconstructed using silicon microstrip detectors [7, 8] and a 96-layer open-cell drift chamber (COT) [9] inside a 1.4 T solenoid. The number of COT layers traversed by a particle in the range $|\eta_{\rm d}| \leq 1$ is 96 and decreases to zero for $|\eta_{\rm d}| \to 2$. The silicon system provides coverage with 6 (7) layers with radii between 2.4 cm and 28 cm for $|\eta_{\rm d}| < 1.0$ ($1.0 < |\eta_{\rm d}| < 2.0$). Outside of the solenoid are electromagnetic (EM) and hadronic (HAD) sampling calorimeters, segmented in a projective tower geometry, and constructed of layers of lead or iron absorber, respectively, and scintillator. The EM section is the first 19-21 radiation lengths (X_0), corresponding to one hadronic interaction length (λ) and contains electromagnetic showers, while the HAD section extends to 4.5-7 λ and contains the majority of a hadronic shower. The calorimeters are divided into central ($|\eta_{\rm d}| < 1.1$) and forward ($1.1 < |\eta_{\rm d}| < 3.64$) regions. Outside of the central calorimeters are muon detectors consisting of scintillators and drift chambers.

Including the leptonic τ decays, the branching fraction of the WZ state to three e or μ leptons is 1.8%. When coupled with the small SM cross section, this implies that only a small number ($\sim$70) of $WZ \to \ell'\nu_{\ell'}\ell\ell$ events are expected to be produced in 1.1 fb^{-1} at the Tevatron. Furthermore, in order to identify a WZ event in this decay channel, all three charged leptons must be detected. The CDF II detector, however, has gaps in calorimeter coverage and limited forward ($|\eta_{\rm d}| \gtrsim 1$) tracking efficiency.

In order to maximize the total acceptance, while minimizing the backgrounds from jets and photons misidentified as leptons, we exploit all available reconstructed tracks and clusters of energy in the EM calorimeter. We separate these into seven non-overlapping lepton categories: three each of electrons and muons, and a seventh for tracks that are non-fiducial to the calorimeters and are not identified as muons. In this context, "non-fiducial" refers to detector regions that are inactive for energy measurement because they are either not covered, or are only partially covered, by calorimeter components.

All lepton candidates are required to be isolated such that the sum of the E_T for the calorimeter towers in a cone of $\Delta R = \sqrt{(\Delta\eta)^2 + (\Delta\phi)^2} < 0.4$ around the lepton is less than 10% of the E_T for electrons or p_T for muons and track lepton candidates. The transverse energy E_T of an energy cluster or calorimeter tower is $E \sin\theta$, where E is the associated energy. Similarly, p_T is the component of track momentum transverse to the beam line.

All electron candidates are required to have a cluster of energy in the calorimeter with the ratio of deposition in the HAD to EM sections consistent with being due to an electron. These candidates are divided into three categories: those in the central calorimeter, those in the forward calorimeter matched to a track, and those in the forward calorimeter without a matched track. The central electron category requires a well-measured COT track. Since the tracking efficiency is low in the large $|\eta_{\rm d}|$ region, a track pattern algorithm which starts with calorimeter information and attempts to attach silicon hits is used for forward electrons. For forward electrons without a matched track, both charge hypotheses are considered when forming WZ candidates, since the charge is determined from the track curvature.

For all muon candidates, the energy deposition in both the EM and HAD calorimeter sections is required to be consistent with that of a minimum ionizing particle. The muon candidates are divided into a category in which the tracks match to reconstructed track segments ("stubs") in the muon chambers and two categories of tracks that do not match to stubs ("stubless"). The stubless muon candidates are designated as central or forward, depending on the calorimeter to which the track is projected.

The stubbed and central stubless muons have strict requirements on the number of COT hits and the χ^2 of the track fit in order to suppress background muons from $K^{\pm}$ or $\pi^{\pm}$ decays. To increase the track finding efficiency in the forward region, we use an algorithm that starts with silicon detector hits in addition to one that starts with COT hits. The forward stubless muons require at least 60% of the traversed COT layers to have hits. To suppress the background from cosmic rays and $K^{\pm}$ or $\pi^{\pm}$ decays, we require the point of closest approach of the track to the beamline to be consistent with having originated from the beam, in addition to using a cosmic ray rejection algorithm.

An additional category consists of tracks that neither project to the fiducial regions of the calorimeters nor are identified as stubbed muons. The requirements for these track-only lepton candidates are the same as for central stubless muons, but without the calorimeter requirements. Due to the lack of calorimeter information, electrons and muons cannot be reliably differentiated for this category, and are therefore treated as having either flavor in the WZ candidate selection. If an electron or track-only candidate is consistent with a photon conversion, as indicated by the presence of an additional nearby track with a common vertex, the candidate is rejected.

To measure the presence of a neutrino, we use missing transverse energy $\not\!\!E_T = |\sum_i E_{T,i}\, \hat{n}_{T,i}|$, where $\hat{n}_{T,i}$ is the transverse component of the unit vector pointing from the interaction point to calorimeter tower i. The $\not\!\!E_T$ calculation is corrected for muons and track-only lepton candidates, which do not deposit all of their energy in the calorimeter.

The events we consider must pass one of four online trigger selections. The events with central electrons require an EM energy cluster with $E_T > 18$ GeV matched to a track with $p_T > 8$ GeV/c. The events with forward electrons require an EM energy cluster with $E_T > 20$ GeV and an uncorrected, calorimeter-based measurement of $\not\!\!E_T > 15$ GeV. Muon triggers are based on stubs from the muon chambers matched to a track with $p_T > 18$ GeV/c. Trigger efficiencies are measured in leptonic W and Z data samples [1].

The WZ candidates are selected from events with exactly three lepton candidates using requirements that were optimized with Monte Carlo simulation without reference to the data. At least one lepton is required to satisfy the trigger and have $E_T > 20$ GeV ($p_T > 20$ GeV/c) for electrons (muons). We loosen this requirement to 10 GeV (GeV/c) for the other leptons to increase the WZ kinematic acceptance. Aside from WZ production, other SM processes that can lead to three high-p_T leptons include dileptons from the Drell-Yan Z/γ^* process (DY), with an additional lepton from a photon conversion ($Z\gamma$) or a misidentified jet (Z+jets) in the event; ZZ production where only three leptons are identified and the unobserved lepton results in $\not\!\!E_T$; and a small contribution from $t\bar{t} \to WbW\bar{b}$, where two charged leptons result from the W boson decays and one or more from decay of the b-quarks. Except for $t\bar{t}$, these backgrounds are suppressed by requiring $\not\!\!E_T > 25$ GeV in the event, consistent with the unobserved neutrino from the leptonic decay of a W boson. We also require the azimuthal angle between the $\not\!\!E_T$ direction and any identified jet with $E_T > 15$ GeV or WZ candidate lepton to be greater than 9° to suppress DY backgrounds in which the observed $\not\!\!E_T$ is due to mismeasured leptons and/or jets.

We require at least one same-flavor, opposite-sign lepton pair in the event with an invariant mass $M_{\ell^+\ell^-}$ in the range [76, 106] GeV/c^2, consistent with the decay of a Z boson. This range is referred to as the "Z-mass region." If there is more than one such pair, the leptons with $M_{\ell^+\ell^-}$ closest to the Z mass [10] are treated as the Z boson decay candidate pair. In order to suppress backgrounds from ZZ, we require that no additional track in the event with $p_T > 8$ GeV/c, when combined with the lepton that is not part of the Z boson decay candidate pair, has an invariant mass in the Z-mass region. The overall acceptance for $WZ \to \ell'\nu_{\ell'}\ell\ell$, using the described selection criteria, is 13.4%.

The acceptances for the WZ, ZZ, $Z\gamma$, and $t\bar{t}$ processes are determined using Monte Carlo calculations followed by a GEANT-based simulation [11] of the CDF II detector. The Monte Carlo generator used for WZ, ZZ, and $t\bar{t}$ is PYTHIA [12] and for $Z\gamma$ is the generator described in [13]. We use the CTEQ5L parton distribution functions (PDFs) to model the longitudinal momentum distribution of the initial-state partons [14]. An efficiency correction, of up to 10% per lepton, is applied to the simulation based on measurements of the lepton reconstruction and identification efficiencies using observed $Z \to \ell^+\ell^-$ events. An additional correction is applied to the $Z\gamma$ background estimate based on a measurement of the photon conversion veto efficiency in data. The background from Z+jets is estimated from a sample of events with two identified leptons and a jet that is required to pass loose isolation requirements and contain a track or energy cluster similar to those required in the lepton identification. The contribution of each event to the total yield is scaled by the probability that the jet is identified as a lepton. This probability is determined from multijet events collected with a set of jet-based triggers. A correction is applied for the small real lepton contribution using single W and Z boson Monte Carlo simulation.

Systematic uncertainties associated with the Monte Carlo simulation affect the $Z\gamma$, ZZ, $t\bar{t}$, and WZ simulations similarly. The uncertainties from the lepton selection and trigger efficiency measurements are propagated through the analysis, giving uncertainties of $1.2\% - 2.0\%$ and $0.4\% - 0.9\%$ for the respective efficiencies of the different signal and background processes. The uncertainty due to the $\not\!\!E_T$ resolution modeling is determined from comparisons of the data and the Monte Carlo simulation

in a sample of dilepton events. For WZ, ZZ, and $t\bar{t}$ production, where it is an observed particle that produces the observed $\not\!\!E_T$, we determined the uncertainty to be 1%. The uncertainty due to the $\not\!\!E_T$ modeling for the $Z\gamma$ background is much larger (25%) than for other final states because it depends on the non-Gaussian tails of the resolution function. The uncertainties on the ZZ, $Z\gamma$, and $t\bar{t}$ cross sections are assigned to be 10% [5], 10% [15], and 15% [16, 17], respectively. For the $Z\gamma$ background contribution, there is an additional uncertainty of 20% from the detector material description and conversion veto efficiency. The detector acceptance variation due to PDF uncertainties is assessed to be 2% using the 20 pairs of PDF sets described in [18]. The systematic uncertainty on the Z+jets background is determined from differences in the measured probability that a jet is identified as a lepton for jets collected using different jet E_T trigger thresholds. These variations correspond to changing the parton composition of the jets and the relative amount of contamination from real leptons. The total systematic uncertainty on the Z+jets background prediction is 23%. The signal and background estimates obtained from simulation have an additional 6% uncertainty originating from the luminosity measurement [19].

In addition to the signal region ($\not\!\!E_T > 25$ and $M_{\ell^+\ell^-}$ in the Z-mass region), we define two independent trilepton control regions, both with $\not\!\!E_T < 25$ GeV, but different $M_{\ell^+\ell^-}$ criteria, to validate our background estimates. The "Z-mass control region" is defined to have $M_{\ell^+\ell^-}$ in the Z-mass region and is dominated by Z+jets and $Z\gamma$ where the photon is from initial-state radiation. The "Z-veto control region" is defined to have $M_{\ell^+\ell^-}$ outside of the Z-mass region and a minimum value for $M_{\ell^+\ell^-}$ of 40 GeV/c^2. This region is dominated by $Z\gamma$ where the photon is from final-state radiation. We expect 243.5 $\pm$ 38.8 (250.9 $\pm$ 48.3) events in the Z-mass (Z-veto) control region and observe 215 (241) events. The results for the trilepton classifications we consider are shown in Table I and are in good agreement with the expectations.

The expectation in the signal region for WZ and each background contribution is summarized in Table II. In this region, we expect 2.7 $\pm$ 0.4 background events and observe 16 events. A breakdown of the observed (expected) events by flavor classification is as follows: 6 (2.7 $\pm$ 0.2) eee, 0 (2.0 $\pm$ 0.2) $ee\mu$, 1 (1.5 $\pm$ 0.1) $e\mu\mu$, 1 (1.2 $\pm$ 0.1) $\mu\mu\mu$, 5 (2.0 $\pm$ 0.2) $ee\ell_t$, 2 (1.3 $\pm$ 0.1) $e\mu\ell_t$, 1 (1.1 $\pm$ 0.1) $\mu\mu\ell_t$, 0 (0.5 $\pm$ 0.1) $e\ell_t\ell_t$, and 0 (0.2 $\pm$ 0.1) $\mu\ell_t\ell_t$. Here ℓ_t denotes the track-only lepton candidates having unknown flavor. The distributions of $\not\!\!E_T$, $M_{\ell^+\ell^-}$, and the W transverse mass $M_T^W \equiv \sqrt{2E_T\not\!\!E_T(1-\cos\phi_{\ell\nu})}$, where $\phi_{\ell\nu}$ is the azimuthal angle between the non-Z candidate lepton and the $\not\!\!E_T$ direction are shown in Fig. 1. The data are in good agreement with the SM prediction.

Due to the unobserved neutrino, events from $WZ \to \ell'\nu_{\ell'}\ell\ell$ are expected to have larger $\not\!\!E_T$ on average than the DY and ZZ backgrounds. We exploit this information by performing a binned maximum likelihood fit for the signal yield using the following $\not\!\!E_T$ bins: $25 < \not\!\!E_T < 45$ GeV and $\not\!\!E_T > 45$ GeV. This binning was chosen to maximize our sensitivity for a WZ observation without reference to the data. We expect 2.0 $\pm$ 0.4 (0.7 $\pm$ 0.1) background events and 6.5 $\pm$ 0.5 (5.9 $\pm$ 0.4) WZ events, with 9 (7) events observed in the lower (upper) $\not\!\!E_T$ bin. We define $\Delta\ln\mathcal{L}$ as the log of the likelihood ratio between this fit and the no signal hypothesis. For our data, we find $2\Delta\ln\mathcal{L} = 37.8$. We interpret this result using 10^{10} background-only Monte Carlo experiments, out of which only 11 had a larger value of $2\Delta\ln\mathcal{L}$ (a probability of 1.1×10^{-9}), corresponding to a significance equivalent to six standard deviations.

This result represents the first observation of WZ production. The measured cross section is

$$\sigma(p\overline{p} \to WZ) = 5.0^{+1.8}_{-1.4}\ (\text{stat.}) \pm\ 0.4\ (\text{syst.})\ \text{pb},$$

consistent with the SM expectation.

We thank the Fermilab staff and the technical staffs of the participating institutions for their vital contributions. This work was supported by the U.S. Department

TABLE I: Summary of the expected and observed yields in the trilepton control regions. In the classification column, ℓ_t denotes a track-only lepton candidate having unknown flavor. The eee, $e\mu\mu$, $ee\ell_t$, and $e\mu\ell_t$ classifications receive a large contribution from $Z\gamma$ events where the photon is reconstructed as a forward electron without a matched track.

Flavor	Z-mass		Z-veto	
Classification	Expected	Data	Expected	Data
$e\ e\ e$	116.3 ± 19.2	103	114.8 ± 22.5	103
$e\ e\ \mu$	1.8 ± 0.3	2	1.4 ± 0.4	4
$e\ \mu\ \mu$	62.5 ± 10.3	50	69.2 ± 14.0	62
$\mu\ \mu\ \mu$	1.1 ± 0.2	1	0.3 ± 0.1	1
$e\ e\ \ell_t$	29.6 ± 4.6	20	33.5 ± 6.2	31
$e\ \mu\ \ell_t$	24.9 ± 4.1	33	26.5 ± 5.2	34
$\mu\ \mu\ \ell_t$	2.7 ± 0.4	5	1.9 ± 0.4	3
$e\ \ell_t\ \ell_t$	4.0 ± 0.7	1	2.6 ± 0.5	2
$\mu\ \ell_t\ \ell_t$	0.4 ± 0.2	0	0.4 ± 0.1	1
Total	243.5 ± 38.8	215	250.9 ± 48.3	241

TABLE II: Expected number of events in the signal region for WZ and the background contributions. "Lumi" refers to the integrated luminosity uncertainty, which is absent for the Z+jets because it is determined from the same dataset.

Source	Expectation ± Stat ± Syst ± Lumi
Z+jets	1.21 ± 0.27 ± 0.28 ± −
ZZ	0.88 ± 0.01 ± 0.09 ± 0.05
$Z\gamma$	0.44 ± 0.05 ± 0.15 ± 0.03
$t\bar{t}$	0.12 ± 0.01 ± 0.02 ± 0.01
Total Background	2.65 ± 0.28 ± 0.33 ± 0.09
WZ	9.75 ± 0.03 ± 0.31 ± 0.59
Total Expected	12.41 ± 0.28 ± 0.45 ± 0.67
Observed	16

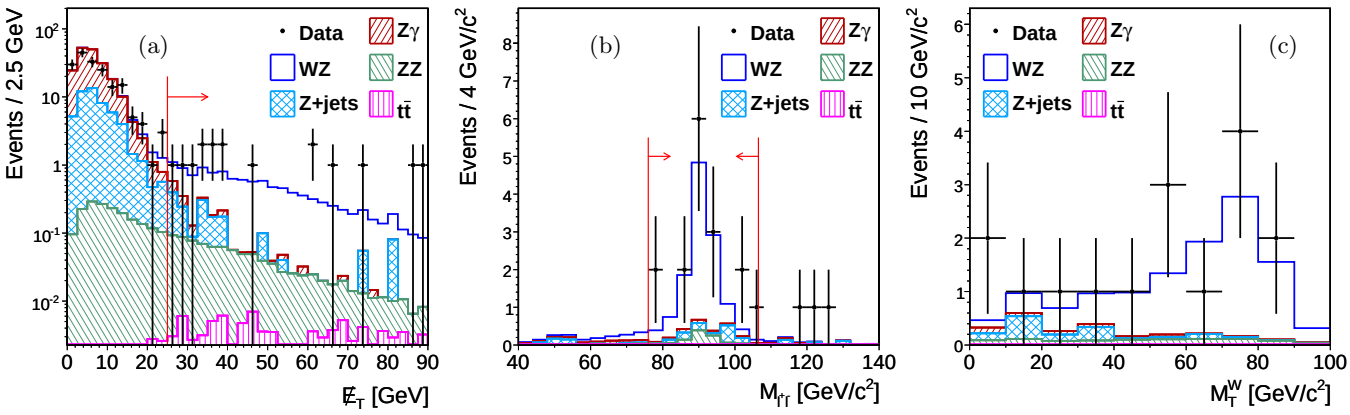

FIG. 1: Distributions for WZ candidates of (a) the $\not\!\!E_T$ (b) the dilepton invariant mass for the same-flavor opposite-sign dilepton pair closest to the Z mass, and (c) the W transverse mass calculated from the remaining lepton and the $\not\!\!E_T$. In (a) and (b), the arrows indicate the signal region.

of Energy and National Science Foundation; the Italian Istituto Nazionale di Fisica Nucleare; the Ministry of Education, Culture, Sports, Science and Technology of Japan; the Natural Sciences and Engineering Research Council of Canada; the National Science Council of the Republic of China; the Swiss National Science Foundation; the A.P. Sloan Foundation; the Bundesministerium für Bildung und Forschung, Germany; the Korean Science and Engineering Foundation and the Korean Research Foundation; the Particle Physics and Astronomy Research Council and the Royal Society, UK; the Institut National de Physique Nucleaire et Physique des Particules/CNRS; the Russian Foundation for Basic Research; the Comisión Interministerial de Ciencia y Tecnología, Spain; the European Community's Human Potential Programme under contract HPRN-CT-2002-00292; and the Academy of Finland.

[1] D. Acosta *et al.* (CDF Collaboration), Phys. Rev. Lett. **94**, 091803 (2005).
[2] K. Hagiwara, S. Ishihara, R. Szalapski, and D. Zeppenfeld, Phys. Rev. D **48**, 2182 (1993).
[3] V. M. Abazov *et al.* (DØ Collaboration), Phys. Rev. Lett. **95**, 141802 (2005).
[4] D. Acosta *et al.* (CDF Collaboration), Phys. Rev. D **71**, 091105 (2005).
[5] J. M. Campbell and R. K. Ellis, Phys. Rev. D **60**, 113006 (1999).
[6] D. Acosta *et al.* (CDF Collaboration), Phys. Rev. D **71**, 032001 (2005).
[7] A. Sill *et al.*, Nucl. Instrum. Methods A **447**, 1 (2000).
[8] A. Affolder *et al.*, Nucl. Instrum. Methods A **453**, 84 (2000).
[9] T. Affolder *et al.*, Nucl. Instrum. Methods A **526**, 249 (2004).
[10] W.-M. Yao *et al.* (Particle Data Group), J. Phys. G **33**, 1 (2006).
[11] R. Brun, R. Hagelberg, M. Hansroul, and J. Lassalle, version 3.15, CERN-DD-78-2-REV.
[12] T. Sjostrand, S. Mrenna, and P. Skands, J. High Energy Phys. **0605**, 026 (2006).
[13] U. Baur and E. L. Berger, Phys. Rev. D **47**, 4889 (1993).
[14] H. L. Lai *et al.* (CTEQ Collaboration), Eur. Phys. J. C **12**, 375 (2000).
[15] U. Baur, T. Han, and J. Ohnemus, Phys. Rev. D **57**, 2823 (1998).
[16] N. Kidonakis and R. Vogt, Phys. Rev. D **68**, 114014 (2003).
[17] M. Cacciari, S. Frixione, M. L. Mangano, P. Nason, and G. Ridolfi, J. High Energy Phys. **0404**, 068 (2004).
[18] S. Kretzer, H. L. Lai, F. I. Olness, and W. K. Tung (CTEQ), Phys. Rev. D **69**, 114005 (2004).
[19] D. Acosta *et al.*, Nucl. Instrum. Methods A **494**, 57 (2002).